Published in final edited form as:

Brain Res. 2016 October 1; 1648(Pt A): 181–192. doi:10.1016/j.brainres.2016.07.035.

Lipopolysaccharide (LPS) and tumor necrosis factor alpha (TNFα) blunt the response of Neuropeptide Y/Agouti-related peptide (NPY/AgRP) glucose inhibited (GI) neurons to decreased glucose

Lihong Hao[1,2], **Zhenyu Sheng**[1], **Joseph Potian**[1], **Adam Deak**[1], **Christine Rohowsky-Kochan**[1], and **Vanessa H. Routh**[1,*]

[1]Department of Pharmacology, Physiology & Neuroscience, New Jersey Medical School, Rutgers University, Newark, NJ, USA

[2]Graduate School of the Biomedical Sciences, New Jersey Medical School, Rutgers University, Newark, NJ, USA

Abstract

A population of Neuropeptide Y (NPY) neurons which co-express Agouti-related peptide (AgRP) in the arcuate nucleus of the hypothalamus (ARC) are inhibited at physiological levels of brain glucose and activated when glucose levels decline (e.g. glucose-inhibited or GI neurons). Fasting enhances the activation of NPY/AgRP-GI neurons by low glucose. In the present study we tested the hypothesis that lipopolysaccharide (LPS) inhibits the enhanced activation of NPY/AgRP-GI neurons by low glucose following a fast. Mice which express green fluorescent protein (GFP) on their NPY promoter were used to identify NPY/AgRP neurons. Fasting for 24 hours and LPS injection decreased blood glucose levels. As we have found previously, fasting increased *c-fos* expression in NPY/AgRP neurons and increased the activation of NPY/AgRP-GI neurons by decreased glucose. As we predicted, LPS blunted these effects of fasting at the 24 hour time point. Moreover, the inflammatory cytokine tumor necrosis factor alpha (TNFα) blocked the activation of NPY/AgRP-GI neurons by decreased glucose. These data suggest that LPS and TNFα may alter glucose and energy homeostasis, in part, due to changes in the glucose sensitivity of NPY/AgRP neurons. Interestingly, our findings also suggest that NPY/AgRP-GI neurons use a distinct mechanism to sense changes in extracellular glucose as compared to our previous studies of GI neurons in the adjacent ventromedial hypothalamic nucleus.

*Corresponding author: Vanessa H. Routh, PhD., Professor Department of Pharmacology, Physiology and Neuroscience Rutgers New Jersey Medical School Newark, NJ 07103. routhvh@njms.rutgers.edu.

Conflict of interest

There is no Conflict of interest.

Keywords

NPY/AgRP neurons; GI neurons; anorexia; fasting; LPS; TNFα

1. Introduction

Energy homeostasis is achieved through neuroendocrine and metabolic control of energy intake, storage, and expenditure (Schwartz et al., 2000). The arcuate nucleus (ARC) of the hypothalamus is critical for integrating peripheral signals of energy status and adjusting food intake and energy balance in order to maintain homeostasis (Woods et al., 2000). In particular, activation of ARC Neuropeptide Y/Agouti-related peptide (NPY/AgRP) neurons during energy deficit increases food intake and decreases energy expenditure (Aponte et al., 2011; Krashes et al., 2011; Stanley et al., 1986; White and Kershaw, 1990). NPY/AgRP neurons are also important for increased hepatic glucose output during fasting (Kuperman et al., 2016; Wang et al., 2014). Approximately 40% of ARC NPY/AgRP neurons are glucose-inhibited (GI) neurons. GI neurons are inhibited at physiological brain glucose levels and activated by decreased extracellular glucose (Fioramonti et al., 2007; Muroya et al., 1999). Previous studies in our lab and others show that fasting increases the expression of the neuronal activity marker, *c-fos*, in NPY neurons (Becskei et al., 2008; Murphy et al., 2009b). Fasting also increases the activation of NPY/AgRP-GI neurons by decreased glucose and enhances hypothalamic NPY release in response to decreased glucose (Murphy et al., 2009b). Activation of GI neurons in low glucose is due to an increase in the activity of the cellular fuel sensor, AMP activated protein kinase (AMPK)(Murphy et al., 2009a). Thus, glucose sensing by ARC NPY/AgRP-GI neurons may play a role in maintaining adequate blood glucose levels during energy deficit.

The endotoxin, lipopolysaccharide (LPS) induces illness anorexia and hypermetabolism leading to muscle wasting (Arsenijevic and Montani, 2015; Arsenijevic D, 2000; Becskei et al., 2008; Duan et al., 2014; Duan et al., 2015). Although chronic sepsis is most frequently associated with hyperglycemia, acute sepsis and LPS-induced endotoxemia can cause hypoglycemia in humans and animals (Feingold et al., 2012; Fischer et al., 1986; Krinsley, 2008; Malouf and Brust, 1985; McCallum et al., 1983; Wilmore, 1977). This hypoglycemic effect is most prevalent in patients undergoing glycemic control (Krinsley, 2008). This is important clinically because hypoglycemia during sepsis is negatively correlated with survival (Fischer et al., 1986; Krinsley, 2008). LPS causes hypoglycemia by inhibiting the gluconeogenic enzyme phosphoenolpyruvate carboxykinase (PEPCK) and decreasing hepatic gluconeogenesis (Feingold et al., 2012; McCallum et al., 1983). NPY/AgRP-GI neurons may play a role in the effects of LPS. For example, LPS blocks fasting-induced c-fos expression in NPY/AgRP neurons (Becskei et al., 2008). Hypothalamic AgRP injections prevent muscle wasting during chronic kidney disease (Cheung and Mak, 2012). Interestingly, hypothalamic AMPK activation prevented the effect of LPS on hepatic PEPCK and glucose production (Santos et al., 2013). Together these data suggest that the effects of LPS on metabolism and glucose homeostasis may be due, in part, to inhibition of NPY/AgRP-GI neurons.

LPS increases the levels of a number of inflammatory cytokine (e.g. interleukin-1 (IL-1), interleukin-6 (IL-6), tumor necrosis factor alpha (TNFα), interferon gamma (INFγ)(Baile et al., 1981; Grossberg et al., 2010; Plata-Salaman et al., 1998; Plata-Salamán et al., 1988). TNFα, but not IL-1 or IL-6, is elevated 24 hours post-LPS injection when AgRP expression is at its nadir and markers of muscle wasting are elevated (Duan et al., 2014; Duan et al., 2015). Moreover, PEPCK expression was not decreased by LPS in TNFα receptor knockout mice suggesting a role for TNFα in LPS-induced hypoglycemia (Feingold et al., 2012). TNFα also suppresses AMPK activity (Steinberg et al., 2006). Based on the evidence linking TNFα with the metabolic and hypoglycemic effects of LPS we hypothesized that LPS and TNFα blunt the enhanced activation of NPY/AgRP-GI neurons in response to decreased glucose which we observed following fasting.

To test this hypothesis, we evaluated the effect of LPS on fasting induced changes in NPY/AgRP-GI neurons using mice in which green fluorescent protein was expressed on the NPY promoter (NPY-GFP mice). The activation of NPY-GI neurons by low glucose was evaluated electrophysiologically in brain slices from fasted mice injected with LPS or after in vitro treatment with TNFα. Blood glucose levels decreased to a greater extent in fasted LPS vs saline-treated mice. As we hypothesized, LPS impaired the enhanced activation of NPY/AgRP-GI neurons by low glucose following fasting. In vitro application of TNFα to NPY/AgRP-GI neurons also blunted their activation in low glucose. Interestingly, our results suggest that NPY/AgRP-GI neurons utilize a distinct glucose sensing mechanism compared to our previously characterized GI neurons in the adjacent ventromedial hypothalamic nucleus (VMN).

2. Results

2.1. LPS injection blunts refeeding and decreases body weight and blood glucose levels

LPS causes anorexia, hypermetabolism and hypoglycemia within 24 hours post injection (Arsenijevic D, 2000; Nandivada et al., 2016; Santos et al., 2013). LPS is most commonly injected intraperitoneally (i.p.) (Anderson et al., 2015; Arsenijevic and Montani, 2015; Arsenijevic D, 2000; Duan et al., 2014; Duan et al., 2015; Felies et al., 2004; Porter et al., 2000); however, Becskei et al found that i.p. but not subcutaneously (s.c.) injected LPS caused significant variation in hypothalamic *cfos* expression (Becskei et al., 2008). This group also determined that a higher dose was needed to achieve the same anorexia following s.c. (40 μg/mouse) vs i.p. (4 μg/mouse) injection. Since we wished to measure hypothalamic *cfos* expression in fasted LPS-treated mice, we utilized the protocol established by this group (Becskei et al., 2008). We first performed a pilot study to confirm that 40 μg/mouse LPS s.c. induced anorexia in our hands. As shown by Becskei et al., s.c LPS injection (Fasted/L) significantly decreased food intake compared to that in saline injected fasted mice (Fasted/S) after 6 h, 12 h and 24 h following refeeding (food intake 24 h refeeding: Fasted/S 5.40 ± 0.28g, n=4; Fasted/L 1.93 ± 0.06g, n=3, $t(5) = 10.32$; $P<0.001$; Figure 1a). The body weight of the LPS injected fasted mice was also decreased following refeeding (body weight gain 24 h refeeding: Fasted/S 2.88 ± 0.29g, n=4; Fasted/L −1.62 ± 0.33g, n=4, $t(6) = 10.25$; $P<0.0001$; Figure 1b).

We next confirmed that this dose and route of administration of LPS reduced blood glucose. Significant effects on blood glucose were observed for both fasting [$F(1,68) = 97.6$; $p<0.0001$] and LPS [$F(1,68) = 42.5$; $p< 0.0001$] as well as an interaction between the two treatments [$F(1,68) = 3.8$; $p = 0.05$]. Fasting significantly decreased blood glucose levels compared to the ad lib fed mice. LPS injection resulted in a further decrease in glucose levels in both the fed and fasted state compared to the saline injected mice with the fasted LPS treated mice having significantly lower glucose than all other groups (Figure 1c).

2.2. LPS prevents fasting induced *c-fos* activation in NPY-GFP mice

Colocalization of the immediate early gene product *c-fos* with GFP in ARC sections from NPY-GFP mice was used to evaluate fasting-induced activation of NPY/AgRP neurons in the presence and absence of LPS. We believe that this is a valid assumption since over 95% of ARC NPY neurons co-express AgRP (Broberger et al., 1998). Thus, the overwhelming number of NPY-GFP neurons will be NPY/AgRP neurons and they will be referred to as such. Significant effects on *cfos* expression in NPY/AgRP neurons were observed for both fasting [$F(1,8) = 74.1$; $p<0.0001$] and LPS [$F(1,8) = 45.7$; $p= 0.0001$] as well as an interaction between the two treatments [$F(1,8) = 64.8$; $p<0.0001$]. As shown in Figure 2**,** 24 hours of fasting increased *c-fos* expression in NPY/AgRP neurons compared to that in fed mice. LPS had no effect on *c-fos* activation in NPY/AgRP neurons in ad lib fed mice; however it completely blocked the fasting stimulated *c-fos* activation in these neurons at the 24 hour time point.

2.3. LPS attenuates the effect of fasting on the glucose sensitivity of NPY/AgRP-GI neurons

NPY/AgRP-GI neurons significantly depolarized and increased their IR as glucose levels decreased from 2.5 to 0.5 or from 2.5 to 0.1 mM in fed and fasted mice treated with LPS or saline (Table 1A). In 0.1 mM glucose, NPY/AgRP-GI neurons were significantly more depolarized in fasted vs fed mice from both LPS and saline-treated groups. However, in 0.5 mM glucose NPY/AgRP-GI neurons differences were observed only in fasted vs fed saline-treated mice. Although the pattern was similar (greater difference between fed and fasted with saline vs LPS treatment), 2 way ANOVA revealed no significant intergroup differences in IR due to baseline variability (Table 1A). Importantly, the magnitude of the membrane potential and IR response to decreased glucose differed significantly between groups. That is, while NPY/AgRP-GI neurons from fasted saline-treated mice depolarized to a significantly greater degree in response to glucose decreases from 2.5 to 0.5 or 0.1mM compared to neurons from fed saline-treated mice, there was no difference in the degree of depolarization in response to either glucose decrease in the fasted vs fed LPS-treated mice. The increase in input resistance in response to both glucose decreases was significantly greater in fasted saline-treated vs LPS-treated mice. Representative whole cell current clamp recordings are shown in Figure 3a–d. The top trace in each panel shows the response of an NPY/AgRP-GI neuron to a glucose decrease from 2.5 mM to 0.1 mM. The bottom trace in each panel shows the response of the same neuron to a glucose decrease from 2.5 mM to 0.5 mM. The bar graphs in Figure 3e–f represent the percent change of membrane potential and IR in response to glucose decreases from 2.5 to 0.1 (e) or 0.5 (f) mM. Statistical data from the 2 way ANOVA are reported in the figure legend. Glucose decreases to 0.5 and 0.1mM

are analogous to changes seen in the brain during fasting and insulin-induced hypoglycemia, respectively (De Vries et al., 2003; Silver and Erecinska, 1994; Silver and Erecinska, 1998). We find that a glucose decrease to 0.5–0.7mM provides a half maximal response to glucose (Murphy et al., 2009b; Song and Routh, 2005; Wang et al., 2004). Thus, these concentration decreases allow us to evaluate glucose sensitivity in response maximal and half maximal glucose concentrations.

2.4. TNFα blocks activation of NPY/AgRP-GI neurons by decreased glucose through a presynaptic mechanism

We next evaluated the effects of TNFα on the glucose sensitivity of NPY/AgRP-GI neurons in vitro. The absolute values for membrane potential and IR in the presence of TNFα are shown in Table 1B. Decreased glucose significantly depolarized NPY/AgRP neurons in the absence but not the presence of TNFα. IR was increased by decreased glucose in both the presence and absence of TNFα (Table 1B). However the magnitude of the IR response was lower in the presence of TNFα. As shown in Figure 4a, TNFα (40 ng/ml) significantly decreased the increase in action potential frequency as well as the percentage change in the IR (right panel) of NPY/AgRP-GI neurons in response to a glucose decrease from 2.5 mM to 0.1 mM (% change of IR without TNFα [black line under trace]: 35±7%; % change of IR with TNFα [gray line]: 21±15%, n=5; $t(4)=2.970$; $p< 0.05$, paired Student's t-test). However, the ability of TNFα to blunt the response of NPY/AgRP-GI neurons to decreased glucose was abolished in the presence of the sodium channel blocker tetrodotoxin (TTX; 500 nM [% change of IR with TNFα +TTX: 43±6%, $t(5)=0.7708$; $p>0.05$ compared to % change of IR in 0.1mM glucose alone: 48±5%, n = 6; paired Student's t-test; Figure 4b]). Since TTX blocks presynaptic action potentials, these data are consistent with a presynaptic site of action for TNFα.

2.5. TNFα suppresses AMPK phosphorylation in low glucose

The VMH contains the ARC and the adjacent VMN. Previous studies on isolated VMH neurons have shown that AMPKα phosphorylation is critical for detection of low glucose by VMH GI neurons (Murphy et al., 2009a; Murphy et al., 2009b). Since TNFα suppresses AMPK activity in skeletal muscle (Steinberg et al., 2006), we hypothesized that TNFα might also blunt VMH AMPKα phosphorylation in response to decreased glucose. As shown in Figure 5, VMH AMPKα phosphorylation increased in response to a glucose decrease from 2.5 mM to 0.1 mM (0.1 mM: 1.7±0.2; 2.5 mM: 1.0±0). As we predicted, lowering glucose in the presence of TNFα blocked this response (0.1 mM+ TNFα: 0.7±0.1). Data were analyzed by one way ANOVA: $F(2,12) = 13.3$; $P<0.001$, n = 5 per group. Group differences were determined by Bonferroni's multiple comparison test. Bars with different letters are statistically different ($P<0.05$). There was no effect of TNFα on total AMPK expression ($F[2,12] = 0.17$; $P=0.84$).

2.6. A distinct glucose sensing mechanism is used by NPY/AgRP-GI neurons

Our previous studies using isolated neurons from the entire VMH or visually identified VMN-GI neurons indicate that activation of VMN-GI neurons in decreased glucose is mediated by AMPKα-induced neuronal nitric oxide synthase (nNOS) activation and the subsequent closure of a chloride channel (Fioramonti et al., 2010; Murphy et al., 2009a;

Song et al., 2001). However, several studies suggest that this may not be true for ARC NPY/AgRP-GI neurons (Leshan et al., 2012; Yang et al., 2011). Moreover, while TNFα prevented AMPKα phosphorylation in low glucose, the effect of TNFα on the glucose sensitivity of NPY/AgRP-GI neurons was via an effect on an upstream presynaptic neuron. These data are not consistent with AMPKα mediated glucose sensing by NPY/AgRP-GI neurons. NPY neurons make up a very small proportion of the total number of VMH-GI neurons. It is possible that our earlier studies using isolated VMH neurons reflect the mechanism underlying glucose sensing by the larger population of VMN-GI neurons without revealing that of the small number of NPY/AgRP neurons present. Thus, we used electrophysiological evaluation of visually identified NPY/AgRP-GI neurons to determine whether AMPKα, nNOS and/or chloride channel closure mediate glucose sensing specifically in this population of GI neurons.

As shown in Figure 6a, the % change of IR of NPY/AgRP-GI neurons in response to decreased glucose persisted in the presence of TTX, which blocks presynaptic action potentials (without TTX: 30±6%; with TTX 26±9%; n=6; $t(5)=0.4723$; $p>0.05$). This suggests that, as for VMN-GI neurons, decreased glucose directly activates NPY/AgRP-GI neurons. Next, we determined whether the glucose sensitive conductance was similar in VMN-GI neurons and NPY/AgRP-GI neurons. The voltage-current relationship showed that the glucose sensitive current reversed at −99.5 mV±5.6 mV (n=6) (Figure 6b). This reversal potential was close to the K^+ rather than Cl^- equilibrium potential in our solutions (E_K= −99.27; E_{Cl}=−51.66). Thus, in NPY/AgRP-GI neurons, the effect of glucose on NPY-GI neurons is mediated by a potassium channel. This suggests that NPY-GI neurons and VMN-GI neurons use different ion channels to respond to changes in extracellular glucose.

To determine whether changes in the activity of intracellular AMPK is a critical component for glucose sensing of NPY/AgRP-GI neurons, the neurons were dialyzed with the AMPK inhibitor Compound C (Cpd C; 10 μM) in the patch pipette solution. 10–15 mins after establishing the whole cell recording configuration to ensure dialysis of Compound C, the glucose sensitivity of NPY/AgRP-GFP neurons was evaluated. Intracellular AMPK inhibition with Compound C did not block the response of NPY/AgRP-GI neurons to decreased glucose (Figure 6c). That is, 5 of 8 NPY/AgRP-GFP neurons (more than 60%) were activated by low glucose with Compound C in the pipette solution. This percentage of NPY/AgRP-GI neurons was what would be expected in the NPY/AgRP population without the inhibitor based on previous studies using cell imaging and whole cell current clamp recordings showing that more than 40% of NPY/AgRP neurons are GI neurons (Fioramonti et al., 2007; Muroya et al., 1999). These data suggest that endogenous AMPK within NPY/AgRP-GI neurons does not mediate glucose sensing. This finding is consistent with the findings of Yang et al., as well as with our observations that although TNFα blunted VMH AMPKα phosphorylation in low glucose, the effect of TNFα on glucose sensing was presynaptic (Yang et al., 2011).

Our previous studies on isolated VMH neurons or electrophysiologically identified VMN-GI neurons have shown that NO production via nNOS was required for activation of VMN-GI neurons by decreased glucose (Canabal et al., 2007; Murphy et al., 2009a). However, when we included the nonspecific NOS inhibitor L-NMMA (0.1 mM) in the pipette solution 75%

of the NPY neurons were still observed to be GI neurons (3 out of 4 neurons; Figure 6d). Moreover, there was no difference in the increase IR of NPY/AgRP-GI neurons as glucose decreased in the presence and absence of L-NMMA (Figure 6e [without L-NMMA: 67±36%; with L-NMMA:54±5%; t(2)=0.3209; n=3; p=0.7787]). This suggests that nNOS is not involved in glucose sensing by NPY/AgRP-GI neurons. This is consistent with data from the Myers laboratory showing that AgRP neurons do not express nNOS (Leshan et al., 2012).

3. Discussion and conclusion

We and others have shown that fasting increases the expression of the neuronal activity marker, *c-fos*, in NPY/AgRP neurons (Murphy et al., 2009b). Fasting also enhances hypothalamic NPY release and activation of NPY/AgRP-GI neurons by decreased glucose (Murphy et al., 2009b). In this study we found that LPS prevented the increased *cfos* activation in NPY/AgRP neurons which we observed 24 hours after LPS injection and food removal. This was associated with a reduction in the response of NPY/AgRP-GI neurons to decreased extracellular glucose. The inflammatory cytokine TNFα similarly reduced the response of NPY/AgRP-GI neurons to decreased glucose. Taken together, our data suggest that the glucose sensing function of NPY/AgRP-GI neurons is a target of disease inflammation and may contribute to impaired energy and glucose homeostasis. Interestingly, we also found that NPY/AgRP-GI neurons may use a distinct glucose sensing mechanism from that which we published previously in VMN GI neurons (Fioramonti et al., 2010; Murphy et al., 2009a; Song et al., 2001).

The arcuate pro-opiomelanocortin (POMC) and NPY/AgRP neurons are critical for maintaining energy homeostasis (Woods et al., 2000). Increased NPY/AgRP neurotransmission during fasting increases food intake, promotes energy storage and decreases energy expenditure in order to restore energy homeostasis (Aponte et al., 2011; Gropp et al., 2005; Hahn TM, 1998; Kalra et al., 1991; Krashes et al., 2011; Luquet et al., 2005). Activation of POMC neurons during energy sufficiency does the converse (Cowley et al., 2001; Mizuno et al., 1999; Parton et al., 2007; Savontaus et al., 2002; Schwartz et al., 2000; Williams et al., 2001). POMC and NPY/AgRP neurons share downstream targets where they act in opposition (Schwartz et al., 2000). AgRP itself is an endogenous melanocortin receptor antagonist and plays a role in peripheral nutrient partitioning during energy deficit (Joly-Amado et al., 2012; Wang et al., 2014; Warne et al., 2013). AgRP neurons are also important for ghrelin- and corticotropin-induced hepatic glucose output during fasting (Kuperman et al., 2016; Wang et al., 2014). We have previously shown that fasting enhances activation of NPY/AgRP-GI neurons by low glucose (Murphy et al., 2009b). This change in glucose sensitivity during fasting could further reinforce the actions of the NPY/AgRP neurons and potentially play a role in ensuring adequate glucose for brain function when energy is limited. Chronic diseases such as cancer and kidney disease are often associated with anorexia and hypermetabolism leading to skeletal muscle wasting (cachexia)(Amitani et al., 2013; Arruda et al., 2010; Braun and Marks, 2010; Braun et al., 2013; Cahlin et al., 2000; Carson and Baltgalvis, 2010). Studies of the underlying mechanism for these metabolic changes have focused primarily on the melanocortin system (Cheung and Mak, 2012; Markison et al., 2005; Marks et al., 2001; Marks et al., 2003;

Sartin JL, 2008; Scarlett et al., 2010). The NPY/AgRP system is less studied. However hypothalamic AgRP injection has been shown to reduce skeletal muscle wasting in a rodent model of chronic kidney disease (Cheung and Mak, 2012). LPS also causes anorexia and hypermetabolism (Arsenijevic and Montani, 2015; Arsenijevic D, 2000). Becskei et al. have shown that LPS blunts fasting-induced *cfos* activation of NPY/AgRP neurons (Becskei et al., 2008). We confirmed this observation and show here that LPS also blunts the fasting enhanced activation of NPY/AgRP-GI neurons in low glucose.

While the preceding data suggest that reduced activity of NPY/AgRP neurons may contribute to the metabolic effects of LPS and inflammation, there are several reports to the contrary. Liu et al. showed that LPS may be acting on the downstream targets of the AgRP neurons as opposed to directly affecting this neuronal population (Liu et al., 2016). Sartin et al. showed that *cfos* actually increased in AgRP neurons 6 hours after LPS injection while Sergeyev et al. showed that NPY expression was unaffected 4 hours post-LPS injection (Sartin JL, 2008; Sergeyev et al., 2001). One possible explanation for the discrepancy is that none of the above studies evaluated the effects of LPS in the fasted state. Moreover, these studies evaluated earlier time points than discussed above. Finally, although McDonald et al. showed that LPS did not block the increased NPY immunolabeling after caloric restriction (MacDonald et al., 2011), this restriction was less severe than an overnight fast. Clearly, further studies are needed to fully understand the role of NPY/AgRP neurons as a target of the metabolic effects of LPS.

It is also possible that the NPY/AgRP-GI neurons play a greater role in the hypoglycemia which can occur in acute sepsis and LPS injection rather than anorexia and hypermetabolism. Such a role is consistent with the glucose sensing function of a subpopulation of these neurons (Fioramonti et al., 2007). This is consistent with our observation that activation of NPY-AgRP-GI neurons was blunted after fasting in LPS-treated mice whose blood glucose levels were reduced compared to saline-treated mice. Although chronic sepsis is most frequently associated with hyperglycemia in humans, there are numerous reports of hypoglycemia especially when sepsis is severe or patients are under glycemic control (Fischer et al., 1986; Krinsley, 2008; Malouf and Brust, 1985; Wilmore, 1977). This is an important clinical issue since hypoglycemia is associated with an increased risk of mortality in these patients (Fischer et al., 1986; Krinsley, 2008; Malouf and Brust, 1985). Sepsis and LPS reduce PEPCK expression leading to decreased hepatic glucose output (Feingold et al., 2012; McCallum et al., 1983). A growing literature suggests a role for NPY/AgRP neurons in triggering hepatic gluconeogenesis and restoring blood glucose after fasting (Könner et al., 2007; Kuperman et al., 2016; Wang et al., 2014). We hypothesize that activation of the NPY/AgRP-GI subpopulation in low glucose mediates this effect. In support of this, AMPK mediates activation of GI neurons in low glucose (Murphy et al., 2009a; Murphy et al., 2009b) and increased hypothalamic AMPK activity blocks the effects of LPS on gluconeogenesis (Feingold et al., 2012).

The effects of LPS on glucose and energy homeostasis appear to be due to a central action of inflammatory cytokines (Becskei et al., 2008; Wisse et al., 2007). For example, the hypermetabolic effect of LPS was absent in mice lacking TNFα while the anorectic effect was absent in mice lacking IFNγ (Arsenijevic D, 2000). On the other hand, Porter et al.

showed that the anorectic effect of LPS was blocked by TNFα inhibition (Porter et al., 2000). Interestingly, both TNFα and IFNγ were elevated 24 hours post-LPS injection (the time point used in the current study) whereas IL-1 and IL-6 were not (Arsenijevic D, 2000). AgRP expression is at its nadir and markers of muscle wasting are elevated at the 24 hour time point (Duan et al., 2014; Duan et al., 2015). ICV injection of IL-1β or TNFα induces anorexia and significantly decreases NPY mRNA expression suggesting that these cytokines may directly or indirectly target NPY/AgRP neurons (Arruda et al., 2010; Gayle et al., 1997). TNFα is also associated with sepsis- and LPS-induced hypoglycemia. For example, LPS suppression of PEPCK is absent in mice lacking TNFα receptors (Feingold et al., 2012). Moreover, TNFα suppresses AMPK activity (Steinberg et al., 2006). In the present study application of TNFα blunted the activation of NPY/AgRP-GI neurons by low glucose. Interestingly, as discussed below, this effect of TNFα was indirect. Taken together, our data are consistent with a role for NPY/AgRP-GI neurons in the impaired glucose and energy homeostasis during endotoxemia.

Unexpectedly, the effect of TNFα on NPY/AgRP-GI neurons was abolished through synaptic isolation with TTX, suggesting that TNFα affects NPY/AgRP-GI neurons indirectly via an action on an upstream neuron. This indirect effect of TNFα may be mediated by the cellular fuel gauge, AMPK. LPS decreased fasting-induced VMH AMPKα activation and TNFα inhibited VMH p-AMPKα in low glucose. This is consistent with data showing that the “hunger” hormone ghrelin excites NPY/AgRP neurons, in part, through changes in presynaptic AMPKα activity (Yang et al., 2011). Therefore, our data and that of others suggest that the effects of LPS on the glucose sensitivity of NPY/AgRP-GI neurons is mediated in part by a presynaptic AMPKα and TNFα-dependent mechanism which counteracts the effects of fasting (Arruda et al., 2010; Murphy et al., 2009a; Yang et al., 2011).

It is important to note that the above conclusion is not consistent with the mechanism for glucose sensing in VMN-GI neurons which we have previously published. That is, using isolated VMH neurons we found that intracellular AMPK activation, nNOS-mediated NO production and Cl^- channel closure are all critical components for glucose sensing by GI neurons (Murphy et al., 2009a). In these studies, it was not possible to discriminate between VMN- and ARC-GI neurons. Therefore, given the relative size of the VMN compared to the ARC, our results were dominated by VMN- rather than ARC-GI neurons. Moreover, while we used electrophysiology to verify our findings in VMN-GI neurons (Fioramonti et al., 2010; Song et al., 2001), we did not confirm this mechanism electrophysiologically in ARC-GI neurons (Murphy et al., 2009a). In the present study, NPY/AgRP neurons were studied directly using NPY-GFP mice. Here we confirm that decreased glucose directly activates NPY-GI neurons; however this activation results from K^+ and not Cl^- channel closure. A similar K^+ channel mediated glucose sensing mechanism has been reported in the NPY neurons from the lateral hypothalamus. Moreover, glucose sensing in the lateral hypothalamic orexin-GI neurons is also K^+ channel dependent (Gonzalez et al., 2008). Consistent with a distinct glucose sensing mechanism for NPY/AgRP-GI neurons, neither the AMPK inhibitor Compound C nor the NOS inhibitor L-NMMA inhibited the response of NPY/AgRP-GI neurons to decreased glucose. Although several studies implicate intracellular AMPK as a nutrient sensor in NPY/AgRP neurons (Kohno et al., 2011;

Mountjoy et al., 2007), the very thorough data of Yang et al. support a presynaptic locus for AMPK (Yang et al., 2011). Moreover, Leshan et al. demonstrated that AgRP neurons do not express nNOS (Leshan et al., 2012). Our data are consistent with these findings and suggest that ARC NPY/AgRP neurons use a distinct mechanism to sense glucose compared to other VMH GI neurons. However, the mechanism by which low glucose closes a K^+ channel in NPY/AgRP-GI neurons remains to be determined.

In conclusion, our data show that fasting enhances activation of NPY/AgRP-GI neurons by low glucose. This is consistent with the hypothesis that NPY/AgRP-GI neurons play a role in sensing decreased glucose during starvation and initiating metabolic processes which increase fuel for the brain. However, LPS significantly attenuates the enhanced response of NPY/AgRP-GI neurons to decreased glucose during fasting. The inflammatory cytokine, TNFα, also blunted the response to low glucose in vitro. These data are consistent with the hypothesis that impaired activation of NPY/AgRP-GI neurons by glucose deficit may contribute to the impaired glucose homeostasis which accompanies sepsis and endotoxemia. Finally, our data emphasize the need to study NPY/AgRP-GI neurons separately from VMN-GI neurons and warrant caution when extrapolating from data obtained using VMH tissue preparations to ARC NPY/AgRP-GI neurons.

4. Experimental Procedure

4.1. Animals

All animal work was approved by the Newark Institutional Animal Care and Use Committee (IACUC) of Rutgers, The State University of New Jersey. 3–6 week old male wild-type C57Bl/6 mice (Charles River) and NPY-GFP mice on a C57Bl/6 background were housed on a 12:12 h light: dark cycle at 22–23°C with food and water available *ad libitum* unless indicated otherwise below.

4.2. LPS injection

Male mice (average body weight 16.6 g) were injected with either vehicle (saline) or LPS (from *Escheria coli 0111:B4* strain, 40 μg/mouse in 0.3ml saline, s.c.). An approximate dose of 4–5 μg/mouse (or 250 μg/kg) LPS given i.p. has been used to cause anorexia and muscle atrophy without inducing severe septic shock (Becskei et al., 2008; Braun and Marks, 2010; Braun et al., 2013). However, Becskei et al. found that an i.p. injection of 4 μg/mouse led to significant variation in *cfos* expression in hypothalamic nuclei, whereas this did not occur with s.c. injection. Furthermore, while 4 μg/mouse given s.c. did not induce anorexia, they found that 40 μg/mouse s.c. led to a similar anorexia as that observed with 4 μg/mouse i.p. (Becskei et al., 2008). Since one of our goals was to evaluate hypothalamic *cfos* expression we chose to follow the protocol used by Becskei et al. Following LPS injection, mice were randomly assigned to either “fed” or “fasted” groups. For the fasted animals, food was removed after injection and mice were fasted for 24 hours (h). Fed animals had food available *ad libitum*. In order to verify the anorectic effect of this dose of LPS, food was returned after 24 hours in a small subpopulation of fasted mice and food intake and body weight was measured after 6 h, 12 h and 24 h post refeeding. The remainder of the fed and fasted animals were sacrificed 24 hours after injection of either saline or LPS.

4.3. Immunohistochemistry

NPY-GFP mice were anesthetized with a lethal dose of pentobarbital (50mg/kg) and transcardially perfused with approximately 15 ml ice cold sterile 0.9% NaCl (with 25U/ml Heparin), followed by 4% paraformaldehyde (PFA) in PBS for around 10 mins. Brains were isolated and post fixed in 4% PFA at 4°C overnight. The brains were then cryoprotected in 30% sucrose in phosphate buffered saline (PBS) at 4°C for 2–3 days, frozen in tissue tech (OCT Embedding Matrix, CellPath, UK) at −20 to −40°C and stored at −80°C. 35μm sections through the VMH were made using a cryostat (Leica) and transferred immediately into a 12 well plate containing 2 ml 1 χ PBS in each well. After washing three times with 1 χ PBS (5 minutes each time), sections were incubated in permeabilization buffer (1 X TBS + 0.1%TWEEN-20 + 0.5% Trition X 100) for 10 mins on a shaker at room temperature, followed by washing three times with 1 X PBS. Sections were then incubated in rabbit antiserum against *fos* protein (1:3000; Ab-5 antibody, Oncogene) overnight at 4°C, washed three times with 1 X PBS and incubated in Alexa Fluor 594 conjugated goat anti-rabbit secondary antibody (1:1000, Invitrogen) for one hour at room temperature. After washing with 1 X PBS, slices were mounted on the slides with ProLong® Gold antifade reagent with DAPI (Invitrogen), covered with coverslips and stored at 4°C for future use. Slices were imaged on a Leica confocal microscope.

4.4. Western blot analysis of AMPK phosphorylation

To study the effect of inflammatory cytokines on AMPK phosphorylation, mice were separated into three groups (5 mice/group). 250 μm brain slices across the ventromedial hypothalamus (VMH), which contains the ARC and VMN, were prepared as described below in **4.5.1.** "**Brain slice preparation".** The VMH was used because sufficient tissue cannot be obtained from the ARC alone. For group 1, brain slices were incubated in 2.5 mM glucose for 30 minutes (mins), and then transferred to 2.5 mM glucose for another 30 mins. For group 2, brain slices were incubated in 2.5 mM glucose for 30 min followed by 0.1 mM glucose for 30 mins. For group 3, brain slices were treated identically to those in group 2; however TNFα (40 ng/ml) was included in the medium. After treatment, the triangular area that surrounds the 3rd cerebral ventricle and contains the VMH neurons was dissected. Western blots were run to determine whether TNFα suppressed VMH AMPK activation in response to decreased glucose.

For Western blots, the VMH was lysed with cell extraction buffer (phenylmethanesulfonylfluoride, Invitrogen and Halt Protease and Phosphatase Inhibitor Cocktails, Thermoscientific). The dissolved proteins were loaded and separated by SDS-PAGE gels. After separation, proteins were transferred to nitrocellulose membranes. Membranes were blocked with 5% milk in Tris-Buffered Saline with 0.1% Tween 20 (TBST) for 1 hour at room temperature. After blocking, membranes were incubated with primary antibodies for phospho-AMPK (anti-AMPKα-Thr 172; 1:500; Cell Signaling) or total AMPK (anti-AMPKα2; 1:1000; Cell Signaling) overnight at 4°C and incubated with relevant secondary antibodies. Target proteins were visualized using SuperSignal West Femto ECL kit. Next, membranes were washed with 1 X TBST for 15 mins and incubated with primary antibodies for β-actin (1:10000; Sigma) in room temperature for 1 hour. After incubation with the appropriate secondary antibodies for half an hour, target proteins were

visualized using SuperSignal West Pico ECL kit (Thermo Scientific, Rockford, IL). Results were presented as the percentage of loading control and normalized to β-actin.

4.5. Brain slice preparation and whole cell current clamp recordings

4.5.1. Brain slice preparation—After anesthetization, NPY-GFP mice were transcardially perfused with ice-cold oxygenated (95% O_2/5% CO_2) perfusion solution: 2.5 mM KCl, 7 mM $MgCl_2$, 1.25 mM NaH_2PO_4, 28 mM $NaHCO_2$, 0.5 mM $CaCl_2$, 7 mM glucose, 1 mM ascorbate, 3 mM pyruvate; osmolarity was adjusted to ~300 mOsm with sucrose; pH 7.4. Coronal sections (300 μm) through the VMH were made on a vibratome (Leica Instruments). Prior to recording, the brain slices were allowed to recover at room temperature for 1 hour in oxygenated artificial cerebrospinal fluid (aCSF; 126 mM NaCl, 1.9 mM KCl, 1.2 mM KH_2PO_4, 26 mM $NaHCO_3$, 2.5 mM glucose, 1.3 mM $MgCl_2$, and 2.4 mM $CaCl_2$; osmolarity was adjusted to ~300 mOsm with sucrose; pH 7.4).

4.5.2. Whole cell current clamp recordings—The standard whole cell recording configuration was established in visually identified NPY-GFP neurons or ARC neurons from wild type mice using an Axopatch 1D amplifier (Axon Instruments, Foster City, CA). Data were analyzed using pClamp9 software. During recording, brain slices were perfused at 6 ml/min with oxygenated aCSF. Borosilicate pipettes (4.0 to 4.5 MΩ) were filled with an intracellular solution containing: 128 mM K-gluconate, 10 mM KCl, 10 mM KOH, 10 mM HEPES, 4 mM $MgCl_2$, 0.05 mM $CaCl_2$, 0.5 mM EGTA, 2 mM Na_2ATP and 0.4 mM Na_2GTP; pH 7.2. Osmolarity was adjusted to 290–300 mOsm with sucrose. Neurons with access resistance more than 35 MΩ during the recording were not used. Input resistance (IR) was calculated according to Ohm's Law (Resistance (R) =Voltage (V)/Current (I)), from the membrane voltage change in response to hyperpolarizing current pulses of −10 or −20 pA. IR was calculated during the last one minute of each glucose or cytokine application. Percentage change of IR and/or membrane potential at 0.1 or 0.5 mM glucose vs 2.5 mM glucose was used to quantitate the data because it is impossible to slice each brain is exactly the same location with respect to synaptic inputs. Therefore, the baseline for these variables can vary significant between neurons. Evaluating the percent change in response to glucose provides a consistent measure of glucose sensitivity between neurons as we have demonstrated previously (Cotero and Routh, 2009; Cotero et al., 2009; Fioramonti et al., 2010; Song et al., 2001; Song and Routh, 2005; Wang et al., 2004). The reversal potential for the glucose sensitive conductance was determined in the current clamp mode using hyperpolarizing pulses from −5 to 50 pA in 5 pA steps. Junction potential was calculated and corrected offline after the recordings.

4.7. Statistical Analysis

The data are presented as mean ± standard error of the mean (SEM). Student's paired or unpaired t-tests or ANOVA (one- or two-way) followed by Tukey's or Bonferroni's multiple comparison test were performed to evaluate group differences, with values of $p<0.05$ considered as significant.

Acknowledgments

This study was supported by NIH R21 CA139063 (VHR).

Abbreviations

3V	3rd cerebral ventricle
AgRP	agouti-related peptide
ARC	arcuate nucleus
Cpd C	Compound C
GI	glucose-inhibited
INFγ	interferon gamma
IL-1	interleukin-1
IL-6	interleukin-6
IR	input resistance
LPS	lipopolysaccharide
ME	median eminence
NPY	neuropeptide Y
PBS	phosphate buffered saline
PFA	paraformaldehyde
TBST	Tris-Buffered Saline with 0.1% Tween 20
TNFα	tumor necrosis factor alpha
TTX	tetrodotoxin
VMN	ventromedial nucleus

References

Amitani M, Asakawa A, Amitani H, Inui A. Control of food intake and muscle wasting in cachexia. The International Journal of Biochemistry & Cell Biology. 2013; 45:2179–2185. [PubMed: 23911307]

Anderson ST, Commins S, Moynagh PN, Coogan AN. Lipopolysaccharide-induced sepsis induces long-lasting affective changes in the mouse. Brain, Behavior, and Immunity. 2015; 43:98–109.

Aponte Y, Atasoy D, Sternson SM. AGRP neurons are sufficient to orchestrate feeding behavior rapidly and without training. Nat Neurosci. 2011; 14:351–355. [PubMed: 21209617]

Arruda AP, Milanski M, Romanatto T, Solon C, Coope A, Alberici LC, Festuccia WT, Hirabara SM, Ropelle E, Curi R, Carvalheira JB, Vercesi AE, Velloso LA. Hypothalamic Actions of Tumor Necrosis Factor α Provide the Thermogenic Core for the Wastage Syndrome in Cachexia. Endocrinology. 2010; 151:683–694. [PubMed: 19996183]

Arsenijevic D, Montani J-P. Uninephrectomy in rats on a fixed food intake potentiates both anorexia and circulating cytokine subsets in response to LPS. Frontiers in Immunology. 2015; 6

Arsenijevic DGI, Vesin C, Vesin D, Arsenijevic Y, Seydoux J, Girardier L, Ryffel B, Dulloo A, Richard D. Differential roles of tumor necrosis factor-alpha and interferon-gamma in mouse hypermetabolic and anorectic responses induced by LPS. European Cytokine Network. 2000; 11:662–668. [PubMed: 11125311]

Baile CA, Naylor J, McLaughlin CL, Catanzaro CA. Endotoxin-elicited fever and anorexia and elfazepam-stimulated feeding in sheep. Physiol Behav. 1981; 27:271–7. [PubMed: 7029576]

Becskei C, Riediger T, Hernadfalvy N, Arsenijevic D, Lutz TA, Langhans W. Inhibitory effects of lipopolysaccharide on hypothalamic nuclei implicated in the control of food intake. Brain Behav Immun. 2008; 22:56–64. [PubMed: 17624718]

Braun T, Marks D. Pathophysiology and treatment of inflammatory anorexia in chronic disease. Journal of Cachexia, Sarcopenia and Muscle. 2010; 1:135–145.

Braun TP, Grossberg AJ, Krasnow SM, Levasseur PR, Szumowski M, Zhu XX, Maxson JE, Knoll JG, Barnes AP, Marks DL. Cancer- and endotoxin-induced cachexia require intact glucocorticoid signaling in skeletal muscle. The FASEB Journal. 2013; 27:3572–3582. [PubMed: 23733748]

Broberger C, Johansen J, Johansson C, Schalling M, Hokfelt T. The neuropeptide Y/agouti gene-related protein (AGRP) brain circuitry in normal, anorectic, and monosodium glutamate-treated mice. Proceedings of the National Academy of Sciences. 1998; 95:15043–15048.

Cahlin C, Körner A, Axelsson H, Wang W, Lundholm K, Svanberg E. Experimental Cancer Cachexia: The Role of Host-derived Cytokines Interleukin (IL)-6, IL-12, Interferon-γ, and Tumor Necrosis Factor α Evaluated in Gene Knockout, Tumor-bearing Mice on C57 Bl Background and Eicosanoid-dependent Cachexia. Cancer Research. 2000; 60:5488–5493. [PubMed: 11034092]

Canabal DD, Song Z, Potian JG, Beuve A, McArdle JJ, Routh VH. Glucose, insulin and leptin signaling pathways modulate nitric oxide (NO) synthesis in glucose-inhibited (GI) neurons in the ventromedial hypothalamus (VMH). AJP - Regulatory, Integrative and Comparative Physiology. 2007; 292:R1418–R1428.

Carson JA, Baltgalvis KA. Interleukin-6 as a Key Regulator of Muscle Mass during Cachexia. Exercise and sport sciences reviews. 2010; 38:168–176. [PubMed: 20871233]

Cheung WW, Mak RH. Melanocortin antagonism ameliorates muscle wasting and inflammation in chronic kidney disease. American Journal of Physiology - Renal Physiology. 2012; 303:F1315–F1324. [PubMed: 22914778]

Cotero VE, Routh VH. Insulin blunts the response of glucose-excited (GE) neurons in the ventrolateral-ventromedial hypothalamic nucleus (VL-VMN) to decreased glucose. AJP - Endocrinology and Metabolism. 2009; 296:E1101–E1109.

Cotero VE, Zhang BB, Routh VH. The Response of Glucose-Excited Neurones in the Ventromedial Hypothalamus to Decreased Glucose is Enhanced in a Murine Model of Type 2 Diabetes Mellitus. J Neuroendocrinol. 2009; 22:65–74. [PubMed: 20002964]

Cowley MA, Smart JL, Rubinstein M, Cerdan MG, Diano S, Horvath TL, Cone RD, Low MJ. Leptin activates anorexigenic POMC neurons through a neural network in the arcuate nucleus. Nature. 2001; 411:480–484. [PubMed: 11373681]

De Vries MG, Arseneau LM, Lawson ME, Beverly JL. Extracellular glucose in rat ventromedial hypothalamus during acute and recurrent hypoglycemia. Diabetes. 2003; 52:2767–2773. [PubMed: 14578295]

Duan K, Yu W, Lin Z, Tan S, Bai X, Gao T, Xi F, Li N. Endotoxemia-induced muscle wasting is associated with the change of hypothalamic neuropeptides in rats. Neuropeptides. 2014; 48:379–386. [PubMed: 25459520]

Duan K, Yu W, Lin Z, Tan S, Bai X, Gao T, Xi F, Li N. Insulin ameliorating endotoxaemia-induced muscle wasting is associated with the alteration of hypothalamic neuropeptides and inflammation in rats. Clinical Endocrinology. 2015; 82:695–703. [PubMed: 25204980]

Feingold KR, Moser A, Shigenaga JK, Grunfeld C. Inflammation inhibits the expression of phosphoenolpyruvate carboxykinase in liver and adipose tissue. Innate Immunity. 2012; 18:231–240. [PubMed: 21450790]

Felies M, von Horsten S, Pabst R, Nave H. Neuropeptide Y stabilizes body temperature and prevents hypotension in endotoxaemic rats. The Journal of Physiology Online. 2004; 561:245–252.

Fioramonti X, Contie S, Song Z, Routh VH, Lorsignol A, Penicaud L. Characterization of glucosensing neuron subpopulations in the arcuate nucleus: Integration in NPY and POMC networks? Diabetes. 2007; 56:1219–1227. [PubMed: 17261674]

Fioramonti X, Marsollier N, Song Z, Fakira KA, Patel RM, Brown S, Duparc T, Pica-Mendez A, Sanders NM, Knauf C, Valet P, McCrimmon RJ, Beuve A, Magnan C, Routh VH. Ventromedial Hypothalamic Nitric Oxide Production Is Necessary for Hypoglycemia Detection and Counterregulation. Diabetes. 2010; 59:519–528. [PubMed: 19934009]

Fischer KF, Lees JA, Newman JH. Hypoglycemia in Hospitalized Patients. New England Journal of Medicine. 1986; 315:1245–1250. [PubMed: 3534567]

Gayle D, Ilyin SE, Plata-Salamán CR. Central Nervous System IL-1β System and Neuropeptide Y mRNAs During IL-1β-induced Anorexia in Rats. Brain Research Bulletin. 1997; 44:311–317. [PubMed: 9323447]

Gonzalez JA, Jensen LT, Fugger L, Burdakov D. Metabolism-Independent Sugar Sensing in Central Orexin Neurons. Diabetes. 2008; 57:2569–2576. [PubMed: 18591392]

Gropp E, Shanabrough M, Borok E, Xu AW, Janoschek R, Buch T, Plum L, Balthasar N, Hampel B, Waisman A, Barsh GS, Horvath TL, Bruning JC. Agouti-related peptide-expressing neurons are mandatory for feeding. Nat Neurosci. 2005; 8:1289–1291. [PubMed: 16158063]

Grossberg AJ, Scarlett JM, Marks DL. Hypothalamic mechanisms in cachexia. Physiol Behav. 2010; 100:478–89. [PubMed: 20346963]

Hahn TMBJ, Baskin DG, Schwartz MW. Coexpression of Agrp and NPY in fasting-activated hypothalamic neurons. Nat Neurosci. 1998; 1:271–272. [PubMed: 10195157]

Joly-Amado A, Denis RGP, Castel J, Lacombe A, Cansell C, Rouch C, Kassis N, Dairou J, Cani PD, Ventura-Clapier R, Prola A, Flamment M, Foufelle F, Magnan C, Luquet S. Hypothalamic AgRP-neurons control peripheral substrate utilization and nutrient partitioning. EMBO J. 2012; 31:4276–4288. [PubMed: 22990237]

Kalra SP, Dube MG, Sahu A, Phelps CP, Kalra PS. Neuropeptide Y secretion increases in the paraventricular nucleus in association with increased appetite for food. Proceedings of the National Academy of Sciences of the United States of America. 1991; 88:10931–10935. [PubMed: 1961764]

Kohno D, Sone H, Tanaka S, Kurita H, Gantulga D, Yada T. AMP-activated protein kinase activates neuropeptide Y neurons in the hypothalamic arcuate nucleus to increase food intake in rats. Neuroscience Letters. 2011; 499:194–198. [PubMed: 21658429]

Könner AC, Janoschek R, Plum L, Jordan SD, Rother E, Ma X, Xu C, Enriori P, Hampel B, Barsh GS, Kahn CR, Cowley MA, Ashcroft FM, Brüning JC. Insulin Action in AgRP-Expressing Neurons Is Required for Suppression of Hepatic Glucose Production. Cell Metabolism. 2007; 5:438–449. [PubMed: 17550779]

Krashes MJ, Koda S, Ye C, Rogan SC, Adams AC, Cusher DS, Maratos-Flier E, Roth BL, Lowell BB. Rapid, reversible activation of AgRP neurons drives feeding behavior in mice. The Journal of Clinical Investigation. 2011; 121:1424–1428. [PubMed: 21364278]

Krinsley JS. The severity of sepsis: yet another factor influencing glycemic control. Critical Care. 2008; 12:1–2.

Kuperman Y, Weiss M, Dine J, Staikin K, Golani O, Ramot A, Nahum T, Kühne C, Shemesh Y, Wurst W, Harmelin A, Deussing Jan M, Eder M, Chen A. CRFR1 in AgRP Neurons Modulates Sympathetic Nervous System Activity to Adapt to Cold Stress and Fasting. Cell Metabolism. 2016; 23:1185–1199. [PubMed: 27211900]

Leshan RL, Greenwald-Yarnell M, Patterson CM, Gonzalez IE, Myers MG. Leptin action through hypothalamic nitric oxide synthase-1-expressing neurons controls energy balance. Nat Med. 2012; 18:820–823. [PubMed: 22522563]

Liu Y, Huang Y, Liu T, Wu H, Cui H, Gautron L. Lipopolysacharide rapidly and completely suppresses AgRP neuron-mediated food intake in male mice. Endocrinology. 2016; 0:en.2015–2081.

Luquet S, Perez FA, Hnasko TS, Palmiter RD. NPY/AgRP Neurons Are Essential for Feeding in Adult Mice but Can Be Ablated in Neonates. Science. 2005; 310:683–685. [PubMed: 16254186]

MacDonald L, Radler M, Paolini AG, Kent S. Calorie restriction attenuates LPS-induced sickness behavior and shifts hypothalamic signaling pathways to an anti-inflammatory bias. American Journal of Physiology - Regulatory, Integrative and Comparative Physiology. 2011; 301:R172–R184.

Malouf R, Brust JCM. Hypoglycemia: Causes, neurological manifestations, and outcome. Annals of Neurology. 1985; 17:421–430. [PubMed: 4004166]

Markison S, Foster AC, Chen C, Brookhart GB, Hesse A, Hoare SRJ, Fleck BA, Brown BT, Marks DL. The Regulation of Feeding and Metabolic Rate and the Prevention of Murine Cancer Cachexia with a Small-Molecule Melanocortin-4 Receptor Antagonist. Endocrinology. 2005; 146:2766–2773. [PubMed: 15774557]

Marks DL, Ling N, Cone RD. Role of the Central Melanocortin System in Cachexia. Cancer Research. 2001; 61:1432–1438. [PubMed: 11245447]

Marks DL, Butler AA, Turner R, Brookhart G, Cone RD. Differential Role of Melanocortin Receptor Subtypes in Cachexia. Endocrinology. 2003; 144:1513–1523. [PubMed: 12639936]

McCallum RE, Seale TW, Stith RD. Influence of endotoxin treatment on dexamethasone induction of hepatic phosphoenolpyruvate carboxykinase. Infection and Immunity. 1983; 39:213–219. [PubMed: 6822414]

Mizuno TM, Makimura H, Silverstein J, Roberts JL, Lopingco T, Mobbs CV. Fasting regulates hypothalamic neuropeptide Y, agouti-related peptide, and proopiomelanocortin in diabetic mice independent of changes in leptin or insulin. Endocrinology. 1999; 140:4551–4557. [PubMed: 10499510]

Mountjoy PD, Bailey SJ, Rutter GA. Inhibition by glucose or leptin of hypothalamic neurons expressing neuropeptide Y requires changes in AMP-activated protein kinase activity. Diabetologia. 2007; V50:168–177. [PubMed: 17093945]

Muroya S, Yada T, Shioda S, Takigawa M. Glucose-sensitive neurons in the rat arcuate nucleus contain neuropeptide Y. Neuroscience Lett. 1999; 264:113–116.

Murphy BA, Fakira KA, Song Z, Beuve A, Routh VH. AMP-activated Protein Kinase (AMPK) and Nitric Oxide (NO) regulate the glucose sensitivity of ventromedial hypothalamic (VMH) glucose-inhibited (GI) neurons. AJP - Cell Physiology. 2009a; 297:C750–C758. [PubMed: 19570894]

Murphy BA, Fioramonti X, Jochnowitz N, Fakira K, Gagen K, Contie S, Lorsignol A, Penicaud L, Martin WJ, Routh VH. Fasting enhances the response of arcuate neuropeptide Y (NPY)-glucose-inhibited (GI) neurons to decreased extracellular glucose. AJP - Cell Physiology. 2009b; 296:746–756.

Nandivada P, Fell GL, Pan AH, Nose V, Ling P-R, Bistrian BR, Puder M. Eucaloric Ketogenic Diet Reduces Hypoglycemia and Inflammation in Mice with Endotoxemia. Lipids. 2016; 51:703–714. [PubMed: 27117864]

Parton LE, Ye CP, Coppari R, Enriori PJ, Choi B, Zhang CY, Xu C, Vianna CR, Balthasar N, Lee CE, Elmquist JK, Cowley MA, Lowell BB. Glucose sensing by POMC neurons regulates glucose homeostasis and is impaired in obesity. Nature. 2007; 449:228–232. [PubMed: 17728716]

Plata-Salaman CR, Ilyin SE, Gayle D, Flynn MC. Gram-negative and gram-positive bacterial products induce differential cytokine profiles in the brain: analysis using an integrative molecular-behavioral in vivo model. Int J Mol Med. 1998; 1:387–97. [PubMed: 9852241]

Plata-Salamán CR, Oomura Y, Kai Y. Tumor necrosis factor and interleukin-1[beta]: suppression of food intake by direct action in the central nervous system. Brain Research. 1988; 448:106–114. [PubMed: 3260533]

Porter MH, Hrupka BJ, Altreuther G, Arnold M, Langhans W. Inhibition of TNF-alpha production contributes to the attenuation of LPS-induced hypophagia by pentoxifylline. AJP - Regulatory, Integrative and Comparative Physiology. 2000; 279:R2113–R2120.

Santos GA, Moura RF, Vitorino DC, Roman EAFR, Torsoni AS, Velloso LA, Torsoni MA. Hypothalamic AMPK activation blocks lipopolysaccharide inhibition of glucose production in mice liver. Molecular and Cellular Endocrinology. 2013; 381:88–96. [PubMed: 23916575]

Sartin JL MD, McMahon CD, Daniel JA, Levasseur P, Wagner CG, Whitlock BK, Steele BP. Central role of the melanocortin-4 receptors in appetite regulation after endotoxin. J Animal Science. 2008; 86:2557–2567.

Savontaus E, Conwell IM, Wardlaw SL. Effects of adrenalectomy on AGRP, POMC, NPY and CART gene expression in the basal hypothalamus of fed and fasted rats. Brain Research. 2002; 958:130–138. [PubMed: 12468037]

Scarlett JM, Bowe DD, Zhu X, Batra AK, Grant WF, Marks DL. Genetic and pharmacologic blockade of central melanocortin signaling attenuates cardiac cachexia in rodent models of heart failure. Journal of Endocrinology. 2010; 206:121–130. [PubMed: 20371568]

Schwartz MW, Woods SC, Porte D, Seeley RJ, Baskin DG. Central nervous system control of food intake. Nature. 2000; 404:661–671. [PubMed: 10766253]

Sergeyev V, Broberger C, Hökfelt T. Effect of LPS administration on the expression of POMC, NPY, galanin, CART and MCH mRNAs in the rat hypothalamus. Molecular Brain Research. 2001; 90:93–100. [PubMed: 11406287]

Silver IA, Erecinska M. Extracellular glucose concentration in mammalian brain: Continuous monitoring of changes during increased neuronal activity and upon limitation in oxygen supply in normo-, hypo-, and hyperglycemic animals. Journal of Neuroscience. 1994; 14:5068–5076. [PubMed: 8046468]

Silver IA, Erecinska M. Glucose-induced intracellular ion changes in sugar-sensitive hypothalamic neurons. J Neurophysiol. 1998; 79:1733–1745. [PubMed: 9535943]

Song Z, Levin BE, McArdle JJ, Bakhos N, Routh VH. Convergence of pre- and postsynaptic influences on glucosensing neurons in the ventromedial hypothalamic nucleus. Diabetes. 2001; 50:2673–81. [PubMed: 11723049]

Song Z, Routh VH. Differential Effects of Glucose and Lactate on Glucosensing Neurons in the Ventromedial Hypothalamic Nucleus. Diabetes. 2005; 54:15–22. [PubMed: 15616006]

Stanley BG, Kyrkouli SE, Lampert S, Leibowitz SF. Neuropeptide Y chronically injected into the hypothalamus: a powerful neurochemical inducer of hyperphagia and obesity. Peptides. 1986; 7:1189–92. [PubMed: 3470711]

Steinberg GR, Michell BJ, van Denderen BJW, Watt MJ, Carey AL, Fam BC, Andrikopoulos S, Proietto J, Gorgun CZ, Carling D, Hotamisligil GS, Febbraio MA, Kay TW, Kemp BE. Tumor necrosis factor [alpha]-induced skeletal muscle insulin resistance involves suppression of AMP-kinase signaling. Cell Metabolism. 2006; 4:465–474. [PubMed: 17141630]

Wang Q, Liu C, Uchida A, Chuang J-C, Walker A, Liu T, Osborne-Lawrence S, Mason BL, Mosher C, Berglund ED, Elmquist JK, Zigman JM. Arcuate AgRP neurons mediate orexigenic and glucoregulatory actions of ghrelin. Molecular Metabolism. 2014; 3:64–72. [PubMed: 24567905]

Wang R, Liu X, Hentges ST, Dunn-Meynell AA, Levin BE, Wang W, Routh VH. The Regulation of Glucose-Excited Neurons in the Hypothalamic Arcuate Nucleus by Glucose and Feeding-Relevant Peptides. Diabetes. 2004; 53:1959–1965. [PubMed: 15277373]

Warne JP, Varonin JM, Nielsen SS, Olofsson LE, Kaelin CB, Chua S, Barsh GS, Koliwad SK, Xu AW. Coordinated Regulation of Hepatic Energy Stores by Leptin and Hypothalamic Agouti-Related Protein. The Journal of Neuroscience. 2013; 33:11972–11985. [PubMed: 23864684]

White JD, Kershaw M. Increased hypothalamic neuropeptide Y expression following food deprivation. Molecular and Cellular Neuroscience. 1990; 1:41–48. [PubMed: 19912753]

Williams G, Bing C, Cai XJ, Harrold JA, King PJ, Liu XH. The hypothalamus and the control of energy homeostasis: different circuits, different purposes. Physiology & Behavior. 2001; 74:683–701. [PubMed: 11790431]

Wilmore DW. Impaired gluconeogenesis in extensively injured patients with gram-negative bacteremia. The American Journal of Clinical Nutrition. 1977; 30:1355–6. [PubMed: 888787]

Wisse BE, Ogimoto K, Tang J, Harris MK Jr, Raines EW, Schwartz MW. Evidence that Lipopolysaccharide-Induced Anorexia Depends upon Central, Rather than Peripheral, Inflammatory Signals. Endocrinology. 2007; 148:5230–5237. [PubMed: 17673516]

Woods SC, Schwartz MW, Baskin DG, Seeley RJ. Food intake and the regulation of body weight. Annu Rev Psychol. 2000; 51:255–77. [PubMed: 10751972]

Yang Y, Atasoy D, Su Helen H, Sternson Scott M. Hunger States Switch a Flip-Flop Memory Circuit via a Synaptic AMPK-Dependent Positive Feedback Loop. Cell. 2011; 146:992–1003. [PubMed: 21925320]

Highlights

- LPS blunted fasting induced activation of NPY/AgRP-GI neurons in response to decreased glucose;
- TNFα blocked the activation of NPY/AgRP-GI neurons by decreased glucose;
- NPY/AgRP-GI neurons use a distinct glucose sensing mechanism from that published previously in adjacent ventromedial hypothalamic GI neurons.

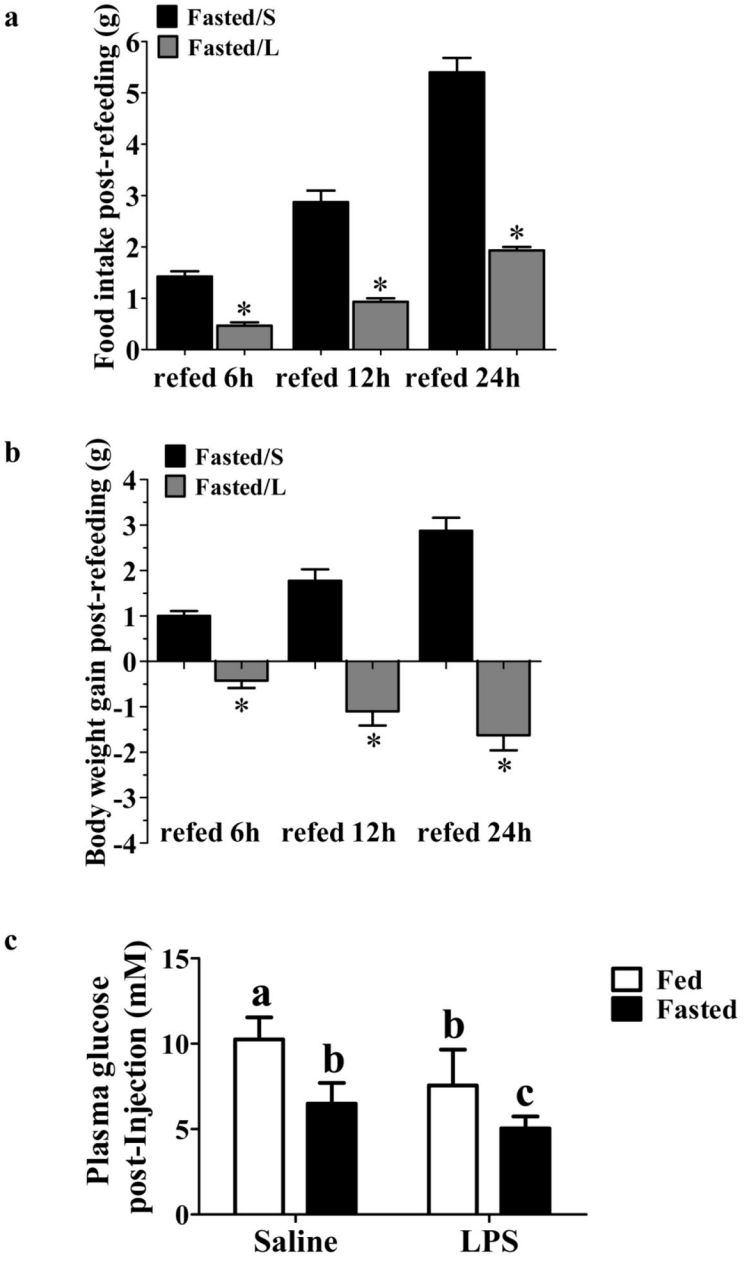

Figure 1. LPS decreased refeeding, body weight and glycemia

(a–b): 4–6 week old male wild-type mice were injected subcutaneously (s.c.) with saline or LPS (40 μg/mouse) prior to food removal. After 24 hours food was returned. Food intake (a) and body weight (b) were measured at 6h, 12h and 24h post-refeeding. LPS decreased food intake and body weight gain at all-time points. Bar graphs represent the food intake or body weight gain post-refeeding at each time point. n=4 for Fasted/S group, n=3 for Fasted/L group. *$p<0.01$ compared to the saline group as determined by student's t-test. (c) 4–6 week old male wild-type mice were separated into fed or fasted groups and injected with saline or LPS (40 μg/mouse, s.c). Food was removed from the fasted groups immediately post-LPS injection. Blood glucose level was measured 24 hours later. Fasting and LPS significantly

decreased blood glucose level, and LPS resulted in a further decrease fasted mice. Different letters indicate statistical significance among the four groups determined by two-way ANOVA followed by Tukey's multiple comparison test ($p<0.05$; Fed/Saline, n=21; Fasted/Saline, n=21; Fasted/LPS, n=21; Fed/LPS, n=9). Bars with the same letter are not statistically different ($p>0.05$).

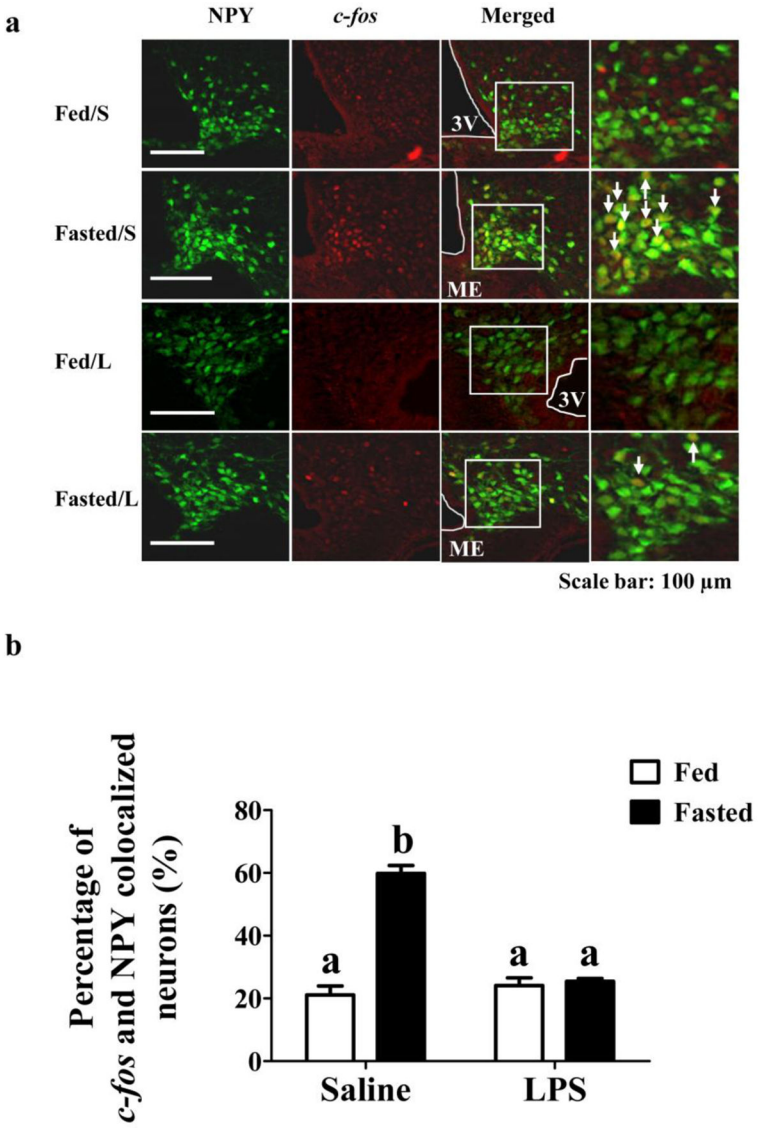

Figure 2. LPS blunted fasting induced *c-fos* activation in NPY-GFP mice

(a) Fasting increased *c-fos* expression in NPY neurons (Fasted/S vs Fed/S); while LPS blocked fasting-induced *c-fos* expression in NPY/AgRP neurons at the 24 hour time point (Fasted/L). LPS had no effect on *c-fos* expression in fed mice (Fed/L). White arrows indicate cells in which NPY/AgRP and *c-fos* are colocalized. (b) Bar graphs represent the percentage of *c-fos* and GFP colocalized cells. Different letters indicate statistical significance among the four groups determined by two-way ANOVA followed by Tukey's multiple comparison test ($p<0.05$; n=3 mice/group).Scale bar: 100 μM. 3V: 3rd cerebral ventricle. Bars with the same letter are not statistically different ($p>0.05$). ME: Median Eminence. The data are presented as mean ± standard error of the mean (SEM).

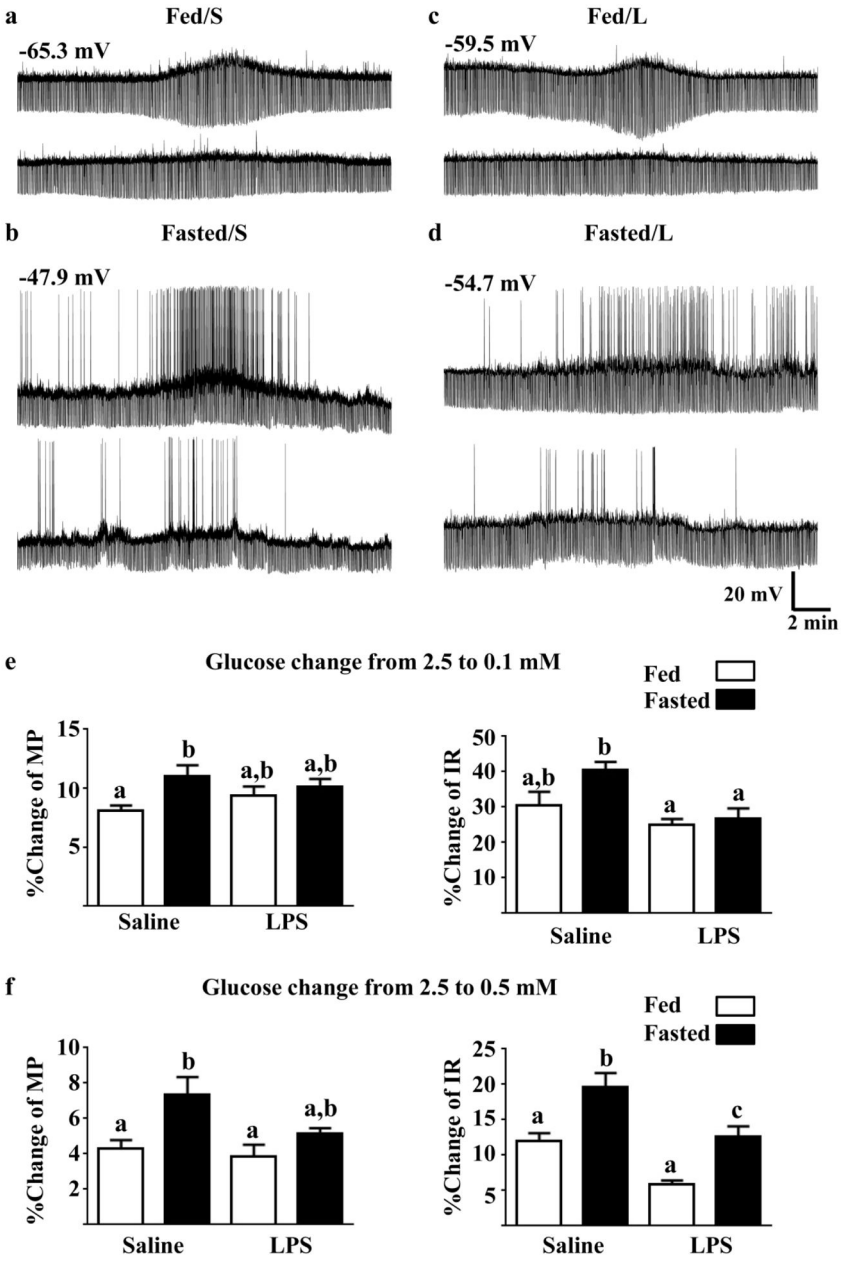

Figure 3. LPS blunted the effect of fasting on the response of NPY-GI neurons to decreased glucose

(a–d) Representative whole cell current-clamp recordings from NPY-GI neurons. The top trace from each of the four groups shows the response of an NPY/AgRP-GI neuron to a glucose decrease from 2.5 mM to 0.1 mM. The bottom trace from each group shows the response of the same neuron to a glucose decrease from 2.5 mM to 0.5 mM. The resting membrane potential is given above the first trace for each group. The percent change of membrane potential and input resistance relative to that in 2.5 mM glucose was used to quantify changes in the response to a glucose decrease from 2.5 to 0.1 (e) and 0.5 mM (f). Data were analyzed by 2 way ANOVA followed by Tukey's multiple comparison test. Different letters represent statistical differences ($p<0.05$; N values ranged from 6–8 neurons

from a minimum of 5 mice for each of the measurements). Bars with the same letter are not statistically different ($p>0.05$). There was a significant increase in depolarization in response to both glucose decreases in the neurons from fasted saline-treated mice compared to fed saline-treated mice. In contrast, the membrane potential response was not enhanced in the fasted vs fed LPS-treated mice. The increase in input resistance in response to decreased glucose was greater in neurons from fasted saline-treated vs LPS-treated mice. The two-way ANOVA results are as follows. Membrane potential 0.1 mM glucose: feeding state $F(1,23) = 7.01$ ($p = 0.01$); treatment $F(1,23) = 0.07$ ($p = 0.79$); interaction $F(1,23) = 2.38$ ($p = 0.13$). Input resistance 0.1 mM glucose: feeding state $F(1,23) = 4.076$ (0.055); treatment $F(1,23) = 10.85$ ($p = 0.003$); interaction $F(1,23) = 2.04$ ($p = 0.16$). Membrane potential 0.5 mM glucose: feeding state $F(1,24) = 10.56$ ($p = 0.003$); treatment $F(1,24) = 3.93$ ($p = 0.06$); interaction $F(1,24) = 1.85$ ($p = 0.19$). Input resistance 0.5 mM glucose: feeding state $F(1,24) = 22.00$ ($p < 0.0001$); treatment $F(1,24) = 26.74$ ($P<0.0001$); interaction $F(1,24) = 0.11$ ($p = 0.74$).

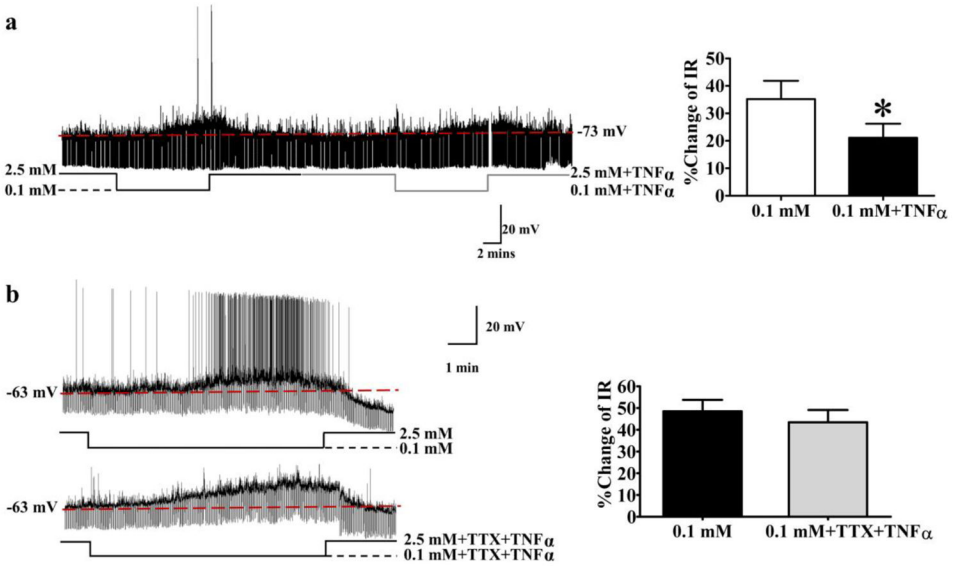

Figure 4. TNFα blunted the response of NPY-GI neurons to decreased glucose through a presynaptic mechanism

Representative current clamp recordings of NPY-GI neurons (a, b; left panels). a) In response to decreased glucose from 2.5 to 0.1 mM, this NPY-GFP neuron depolarized and increased its input resistance (IR; left panel). TNFα attenuated depolarization and increased IR of this NPY-GI neuron in response to decreased glucose. The bar graph shows %change of IR compared to that in 2.5 mM glucose (right panel). *$p<0.05$, determined by paired student's t-test; n=5 neurons evaluated in the presence and absence of TNFα. b) In the presence of the sodium channel blocker tetrodotoxin (TTX), the effect of TNFα on the % change of IR was abolished. n=6 neurons evaluated for an effect of TNFα in the presence and absence of TTX. ns: no significant difference, determined by paired student's t-test ($p<0.05$). The data are presented as mean ± standard error of the mean. Neurons were obtained from 4 – 5 different mice for each experiment.

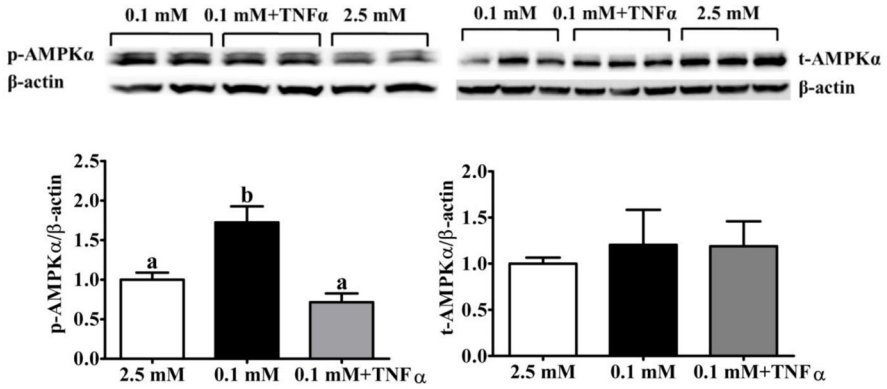

Figure 5. TNFα suppressed VMH AMPKα phosphorylation

VMH slices were exposed to decreased glucose from 2.5 to 0.1 mM in the presence or absence of TNFα (40 ng/ml) for 30 mins. Control slices were maintained in 2.5 mM. Decreasing the glucose concentration increased p-AMPKα; this was blocked by TNFα. t-AMPKα was not affected by low glucose or TNFα ($p<0.05$; n=5 mice/group). Representative western blots are shown at the top and bar graphs representing group averages are shown at the bottom of the figure. Results were presented as the percentage of loading control by normalization to β-actin. The data are presented as mean ± standard error of the mean (SEM). Note that the groups in the representative blot do not follow the order of the bar graph. SEM).

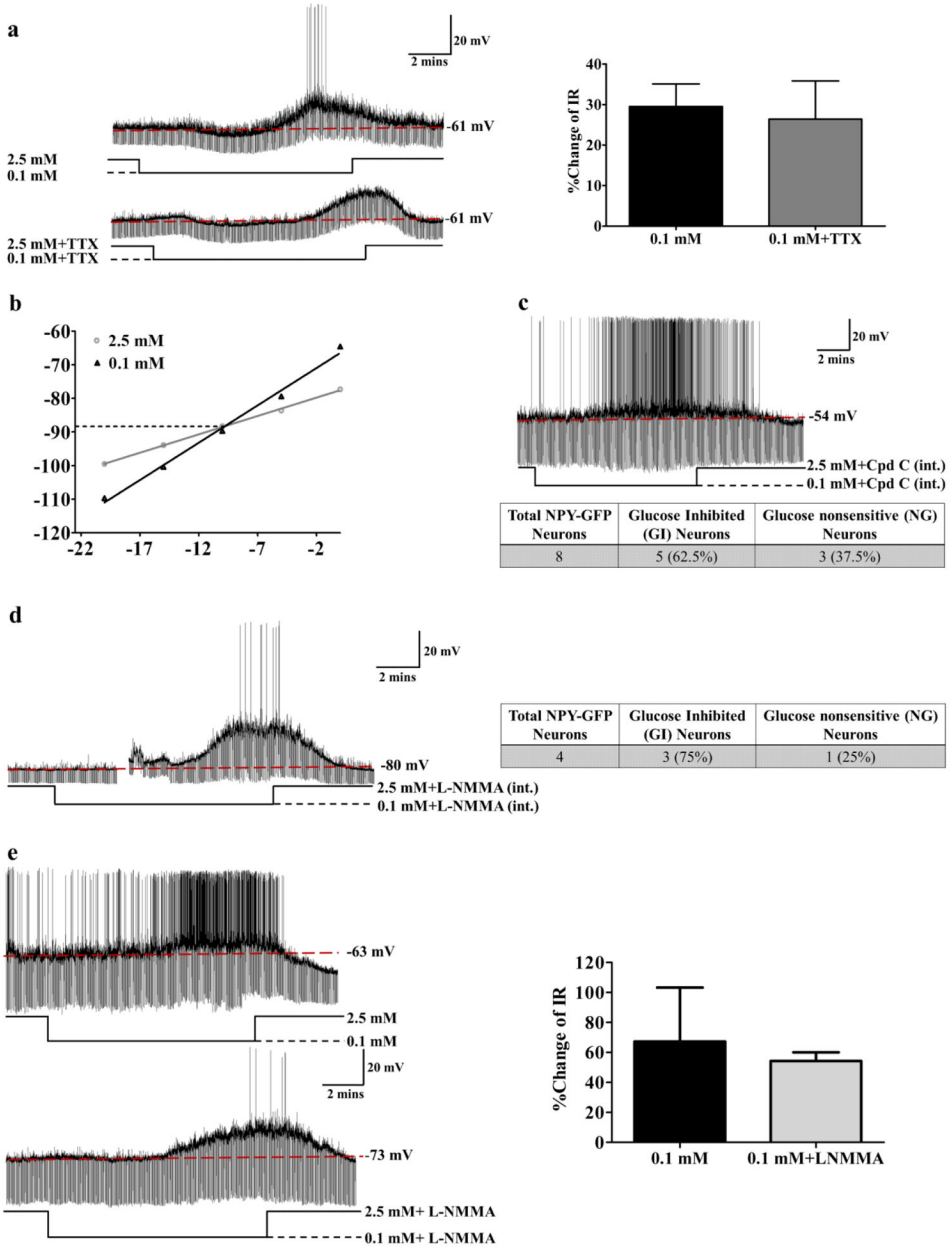

Total NPY-GFP Neurons	Glucose Inhibited (GI) Neurons	Glucose nonsensitive (NG) Neurons
8	5 (62.5%)	3 (37.5%)

Total NPY-GFP Neurons	Glucose Inhibited (GI) Neurons	Glucose nonsensitive (NG) Neurons
4	3 (75%)	1 (25%)

Figure 6. NPY-GI neurons use a distinct glucose sensing mechanism

(a) There was no significant difference in the increased IR in response to decreased glucose from 2.5 to 0.1 mM in the presence or absence of TTX suggesting that low glucose directly activates NPY-GI neurons. The traces are representative whole cell current clamp recordings from an NPY-GI neuron in a brain slice. TTX blocks action potentials as shown in lower trace. The bar graphs represent %change of IR compared to that in 2.5 mM glucose (ns: no significant difference, determined by paired student's t-test; n=6 neurons from 6 different mice evaluated for the effect of 0.1 mM glucose in the presence and absence of TTX). The data are presented as mean ± standard error of the mean (SEM). (b) Hyperpolarizing pulses from −5 to −50 pA in −5 pA steps were injected in 2.5 mM glucose and at the end of each

treatment with 0.1 mM glucose. The membrane voltage measured at each pulse was used to plot the voltage-current relationship. A representative voltage-current relationship is shown. The reversal potential for this NPY-GI neurons is around −89 mV which is close to the potassium equilibrium potential (EK=−99.27) in our solutions. (c) Dialysis of NPY-GFP neurons with Compound C (Cpd C) in the patch pipette solution did not block the response of NPY neurons to decreased glucose. The trace represents the response of an NPY-GI neuron to decreased glucose after intracellular dialysis with the AMPK inhibitor Compound C. Approximately 60% (5 out of 8) of NPY neurons were recorded to be GI neurons (2 mice) after dialysis with intracellular Compound C (int.). This is identical to the expected percentage of NPY-GI neurons in the untreated population (d) Dialysis of an NPY/AgRP-GFP neuron with L-NMMA in pipette solution did not abolish the response of the NPY/AgRP neuron to decreased glucose from 2.5 mM to 0.1 mM. As shown in the table, 3 of 4 NPY/AgRP-GFP neurons (75%; 3 mice) were activated by low glucose after dialysis with intracellular L-NMMA (int.). This is similar to the expected percentage of NPY-GI neurons in the untreated population. The gap in the trace is a mechanical artifact. (e) Bath application of L-NMMA (0.1 mM) did not block the response of this NPY/AgRP-GI neuron to decreased glucose. The bar graphs represent %change of IR compared to that in 2.5 mM glucose. There is no significant difference in the % change IR in response to low glucose in the presence and absence of L-NMMA (n=3 neurons from 3 mice).

Table 1A

Membrane Potential and Input Resistance in 2.5, 0.5 and 0.1 mM glucose for NPY/AgRP GI neurons from fed and fasted mice treated with LPS or saline.

Group	2.5 mM[a]	0.1 mM	P	t (df)	2.5 mM[b]	0.5 mM	P	t(df)
Membrane Potential (mV)								
Fed Saline	−60.4 ± 1.4[a]	−55.7 ± 1.6[a]	<0.0001	t(6)=14.5	−64.5 ± 2.4[a]	−61.5 ± 2.5[a]	0.001	t(5) = 6.8
Fasted Saline	−53.1 ± 1.6[a,b]	−47.3 ± 1.8[b,c]	<0.0001	t(5)=15.8	−53.2 ± 3.1[b]	−49.5 ± 3.3[b,c]	<0.0001	t(6) = 9.7
Fed LPS	−58.1 ± 1.5[a]	−52.6 ± 1.6[a,b]	<0.0001	t(6)=10.9	−56.9 ± 1.3[a,b]	−54.7 ± 1.4[a,b]	0.0005	t(6)=6.8
Fasted LPS	−48.0 ± 2.6[b]	−43.1 ± 2.4[c]	<0.0001	t(6)=13.8	−51.7 ± 1.9[b]	−49.0 ± 1.9[b,c]	<0.0001	t(7) =22.4
Input Resistance (MΩ)								
Fed Saline	1074 ± 84	1387 ± 99	<0.0001	t(6)=12.8	1070 ± 210	1173 ± 144	0.01	t(5)=3.9
Fasted Saline	1220 ± 112	1642 ± 180	0.0083	t(5)=4.2	1206 ± 127	1417 ± 179	0.0098	t(6)=3.7
Fed LPS	1194 ± 106	1481 ± 123	0.0002	t(6)=7.9	1264 ± 100	1334 ± 104	0.0002	t(6)=8.0
Fasted LPS	1115 ± 98	1405 ± 124	0.0005	t(6)=6.9	1130 ± 97	1274 ± 109	0.0002	t(7)=6.9

Data represent Mean ± SEM. Each neuron in each row-group was sequentially evaluated in 2.5 mM glucose (a), 0.1 mM, 2.5 mM glucose (washout, b) and 0.5 mM glucose. Statistical analysis for comparison between 0.1 or 0.5 mM glucose and the preceding exposure to 2.5 mM glucose was done by paired Students t-test. Group differences at each glucose concentration were analyzed by 2 way ANOVA followed by Tukey's multiple comparison test. Groups within columns with different letters are statistically different ($P<0.05$). For membrane potential, the P values and F statistics are as follows: 2.5 mM(a) Feeding State P = 0.0001, F(1,23) = 21.76, Treatment P =0.0593, F(1,23) = 3.94, Interaction P = 0.4604, F(1,23)=0.56; 0.1 mM Feeding State P = 0.0001, F(1,23) = 22.34, Treatment P =0.0663, F(1,23) = 3.72, Interaction P = 0.7741, F(1,23)=0.08; 2.5 mM (b) Feeding State P = 0.0013, F(1,23) = 13.27, Treatment P =0.0547 F(1,23) = 4.08, Interaction P = 0.1919, F(1,23)=1.80; 0.5 mM Feeding State P = 0.001, F(1,23) = 14.01, Treatment P =0.1357, F(1,23) = 2.38, Interaction P = 0.1953, F(1,23)=1.78. There were no group differences for input resistance.

Table 1B

Membrane Potential and Input Resistance in 2.5 and 0.1 mM glucose in the presence and absence of TNFα.

Treatment	2.5 mM	0.1 mM	P	t(df)	2.5 mM +TNFα	0.1 mM +TNFα	P	t(df)
Membrane Potential (mV)	−61.2 ± 1.7	−57.6 ± 1.3	0.042	t(4)=3.0	−67.6 ± 2.0	−65.4 ± 2.6	0.077	t(4)=2.4
Input Resistance (MΩ)	1150 ± 257	1532 ± 314	0.015	t(4)=4.1	915 ± 155	1104 ± 185	0.011	t(4)=4.5

Data represent Mean ± SEM. Neurons were sequentially exposed to 2.5 mM glucose, 0.1 mM glucose, 2.5 mM glucose (washout), 2.5 mM glucose + TNFα and 0.1 mM glucose + TNFα. Statistical analysis was done by paired Students t-test for the response in 2.5 and 0.1 mM G in the presence and absence of TNFα.